Synthesis, Structures, and Thermal and Magnetic Properties of New Coordination Polymers Based on Mn(II) and Ni(II) Thiocyanato Complexes with *trans*-1,2-Bis(4-pyridyl)ethylene as Ligand

Susanne Wöhlert, Inke Jess, and Christian Näther

Institut für Anorganische Chemie der Christian-Albrechts-Universität zu Kiel, Max-Eyth-Straße 2, 24118 Kiel, Germany

Reprint requests to Prof. Dr. Christian Näther. Email: cnaether@ac.uni-kiel.de

Z. Naturforsch. **2012**, *67b,* 41 – 50; received December 1, 2011

Hydrothermal reaction of manganese(II) thiocyanate with *trans*-1,2-bis(4-pyridyl)ethylene (bpe) in water leads to the formation of the new ligand-rich 1 : 3 (ratio metal/ligand) compound $[Mn(NCS)_2(bpe)_2 \cdot (bpe)]$ (**1-Mn**). In the crystal structure the manganese cations are octahedrally coordinated by two thiocyanato anions and four bpe ligands and are linked into layers by the bpe ligands. Reaction of manganese(II) thiocyanate with bpe in water leads to the known 1 : 2 compound $Mn(NCS)_2(bpe)_2(H_2O)_2$ (**2-Mn**). On heating compound **1-Mn** is transformed directly into a ligand-deficient 1 : 1 compound of composition $[Mn(NCS)_2(bpe)]_n$ (**4-Mn**), whereas on thermal decomposition of **2-Mn** a new 1 : 2 anhydrate of composition $[Mn(NCS)_2(bpe)_2]_n$ (**3-Mn**) can be isolated in the first step, which is transformed into **4-Mn** on further heating. In further experiments single crystals of the ligand-deficient compound **4-Mn** were also obtained. In its crystal structure the manganese cations are connected by the thiocyanato anions into Mn-$(NCS)_2$-Mn double chains, which are further connected by bpe ligands into layers. In contrast, reaction of nickel(II) thiocyanate with bpe leads always to the formation of only one crystalline phase (**1-Ni**) that is isotypic to **4-Mn**. Magnetic measurements have revealed that all compounds show Curie or Curie-Weiss paramagnetism.

Key words: Thermal Decomposition, Magnetic Properties, *trans*-1,2-Bis(4-pyridyl)ethylene, Coordination Polymers, Manganese, Nickel

Introduction

Recently, the synthesis, structures and properties of new coordination polymers, metal-organic frameworks (MOFs) or inorganic-organic hybride compounds have attracted much interest because of their diverse physical properties and the potential for future applications of these materials [1 – 4]. Based on simple considerations concerning the coordination behavior of the cations and the ligands, the topology of the coordination networks of such compounds can be influenced to some extent. This can be of some advantage if compounds need to be prepared that show, *inter alia*, cooperative magnetic phenomena. In this case paramagnetic metal centers must be linked by small-sized ligands, which are able to mediate magnetic exchange interactions. Consequently, a number of new coordination compounds on the basis of, *e. g.*, azides or oxalates have been reported that show antiferro- or ferromagnetic ordering [5 – 8]. In this context transition metal thio- or selenocyanato coordination polymers are of interest because they also can mediate magnetic exchange interactions [9 – 13]. However, it must be noted that in most compounds the thiocyanato anions are only terminally coordinated and that the 1,3-bridging mode is less frequently observed [14]. Therefore, the compounds with terminal anions can easily be prepared whereas μ-1,3-bridging thiocyanato coordination compounds cannot always be obtained if the synthesis is performed in the liquid phase. This is unfortunate, because especially these compounds are potential candidates for the occurrence of cooperative magnetic phenomena.

Recently our group presented an alternative and elegant approach to the phase-pure synthesis of new coordination polymers with μ-1,3-bridging thio- and selenocyanato anions, in which octahedrally coordinated ligand-rich precursor compounds with terminal anions and additional neutral co-ligands are heated (ligand-rich = rich in co-ligands). In most cases the co-ligands are removed stepwise, which leads to the formation of ligand-deficient intermediates (ligand-deficient = lack-

ing co-ligands) in which the thio- or selenocyanato anions become μ-1,3-bridging. This structural transformation is frequently accompanied by a dramatic change in the magnetic properties. Whereas most of the ligand-rich compounds exhibit only Curie-Weiss paramagnetism, cooperative magnetic phenomena are frequently observed in the ligand-deficient intermediates [15 – 23]. It must be noted that some of these compounds are not accessible by a reaction of their educts in solution, but they can practically always be prepared phase-pure by thermal decomposition of their corresponding ligand-rich precursors. Later we have also shown that other compounds based on *e. g.* transition metal formates or dicyanamides can be prepared by this route [15, 17].

In order to investigate the correlation between structure, thermal reactivity and magnetic properties of the target compounds in more detail, we started systematic investigations on this topic. Within this project we also investigated coordination polymers based on cobalt(II) thiocyanate with *trans*-1,2-bis(4-pyridyl)-ethylene (bpe) as a ligand and we have found single-chain magnetic behavior for the ligand-deficient 1 : 1 compound with μ-1,3-bridging anions [24]. To prove if the corresponding coordination compounds based on Mn and Ni show a similar thermal reactivity, and if ligand-deficient intermediates can be isolated upon thermal decomposition, we have prepared appropriate precursor compounds and investigated their structural, thermal, spectroscopic and magnetic properties.

Results and Discussion

*Crystal structure of [Mn(NCS)$_2$(bpe)$_2$·(bpe)] (**1-Mn**)*

The reaction of $Mn(NCS)_2 \cdot H_2O$ and *trans*-1,2-bis(4-pyridyl)ethylene (bpe) in the molar ratio 1 : 6 under hydrothermal conditions leads to the formation of single crystals of a ligand-rich 1 : 3 compound [Mn(NCS)$_2$(bpe)$_2$·(bpe)] (**1-Mn**) (bpe = *trans*-1,2-bis(4-pyridyl)ethylene) (see Experimental Section).

Compound **1-Mn** crystallizes in the centrosymmetric space group $P\bar{1}$ with four formula units in the unit cell. The asymmetric unit consists of two Mn^{2+} cations, four thiocyanato anions and five bpe ligands in general positions as well as two bpe ligands located on a center of inversion (Fig. 1). In the crystal structure the two crystallographically independent manganese cations are each coordinated by two terminally *N*-bonded thiocyanato anions and four bridging *N*,*N*′-bonded bpe ligands in an octahedral coordination mode.

Table 1. Selected bond lengths (Å) and angles (deg) for compound **1-Mn**.

Mn1–N13	2.174(4)	Mn2–N15	2.142(4)
Mn1–N14	2.177(4)	Mn2–N16	2.160(4)
Mn1–N2	2.285(3)	Mn2–N21	2.285(4)
Mn1–N62	2.312(3)	Mn2–N41	2.320(3)
Mn1–N61	2.326(3)	Mn2–N42	2.328(3)
Mn1–N1	2.342(3)	Mn2–N22	2.356(4)
N13–Mn1–N14	177.54(14)	N15–Mn2–N16	176.99(15)
N13–Mn1–N2	88.91(13)	N15–Mn2–N21	94.19(14)
N14–Mn1–N2	88.76(13)	N16–Mn2–N21	88.53(13)
N13–Mn1–N62	90.74(12)	N15–Mn2–N41	89.17(12)
N14–Mn1–N62	89.96(12)	N16–Mn2–N41	92.24(12)
N2–Mn1–N62	87.47(12)	N21–Mn2–N41	87.63(12)
N13–Mn1–N61	89.93(12)	N15–Mn2–N42	90.09(12)
N14–Mn1–N61	89.34(12)	N16–Mn2–N42	88.63(12)
N2–Mn1–N61	91.76(12)	N21–Mn2–N42	89.65(12)
N62–Mn1–N61	178.97(12)	N41–Mn–N42	177.12(13)
N13–Mn1–N1	90.55(13)	N15–Mn2–N22	89.54(13)
N14–Mn1–N1	91.79(13)	N16–Mn2–N22	87.76(13)
N2–Mn1–N1	179.15(12)	N21–Mn2–N22	176.21(12)
N62–Mn1–N1	91.88(11)	N41–Mn2–N22	91.76(12)
N61–Mn1–N1	88.90(11)	N42–Mn2–N22	91.01(12)

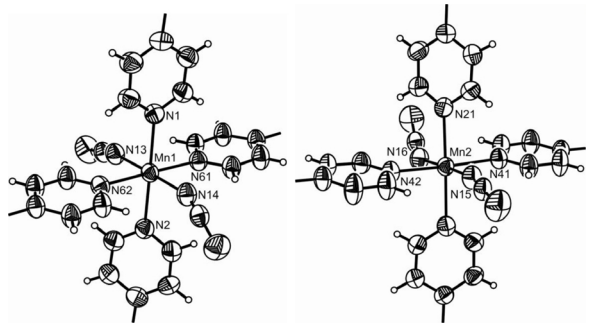

Fig. 1. View of the coordination spheres of the two independent Mn^{2+} cations in the crystal structure of complex **1-Mn** with atom labeling scheme adopted and displacement ellipsoids drawn at the 50 % probability level (ORTEP). For clarity only one half of each bpe ligand is shown.

Both MnN_6 octahedra are markedly distorted with four long Mn–N_{bpe} bonds between 2.285(3) and 2.342(3) Å, two short Mn–NCS bonds of 2.174(4) and 2.177(4) Å for Mn1 as well as four long Mn–N_{bpe} bonds between 2.285(4) and 2.356(4) Å and two short Mn–NCS bonds of 2.142(4) and 2.160(4) Å for Mn2 (Table 1).

The manganese centers are connected by the bpe ligands into linear Mn-bpe-Mn chains that are further linked by the co-ligands into layers (Fig. 2). These layers are stacked onto each other forming channels in which the additional bpe ligands are located.

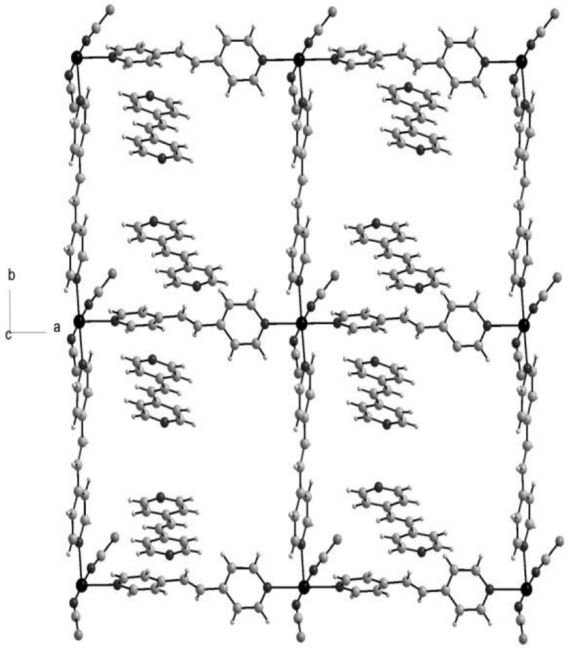

Fig. 2. View of the crystal structure of compound **1-Mn** approximately along the crystallographic *c* axis.

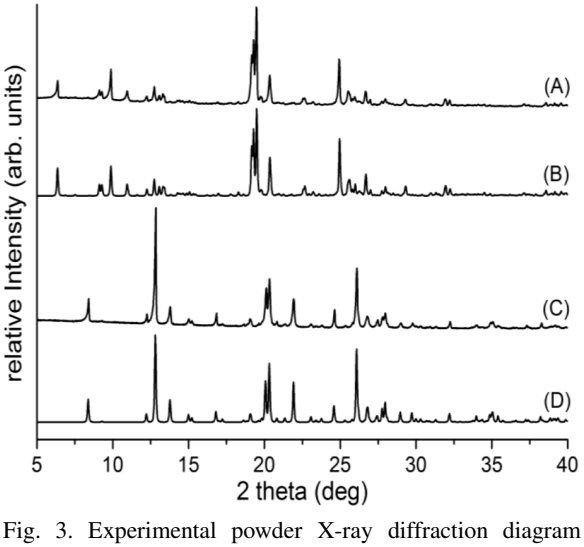

Fig. 3. Experimental powder X-ray diffraction diagram of $[Mn(NCS)_2(bpe)_2 \cdot (bpe)]$ (A) and of $Mn(NCS)_2(bpe)_2(H_2O)_2$ (C) together with the calculated powder X-ray diagrams for **1-Mn** (B) and **2-Mn** (D).

Crystalline powder of **1-Mn** can easily be obtained at r. t., and a comparison of the experimental pattern with that calculated from single-crystal data has proven that this compound is obtained phase-pure (Fig. 3: A and B).

In further experiments a second precursor of composition $Mn(NCS)_2(bpe)_2(H_2O)_2$ (**2-Mn**) was also obtained phase-pure, as proven by the experimental powder pattern of this compound and its comparison with that calculated based on the crystal data reported recently (Fig. 3: C and D and Experimental Section) [25].

Thermal properties

In order to find out if ligand-deficient intermediates can be prepared on heating, the ligand-rich 1 : 3 compound $[Mn(NCS)_2(bpe)_2 \cdot (bpe)]$ (**1-Mn**) as well as

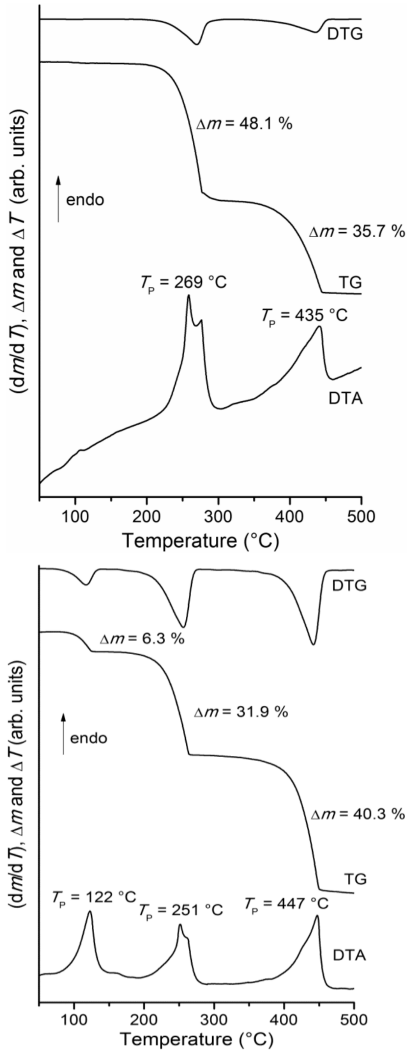

Fig. 4. DTG, TG and DTA curves of $[Mn(NCS)_2(bpe)_2 \cdot (bpe)]$ (**1-Mn**) (top) and $Mn(NCS)_2(bpe)_2(H_2O)_2$ (**2-Mn**) (bottom). [Heating rate = 4 K min^{-1}, N_2 atmosphere, crucible: Al_2O_3, T_P = peak temperature (°C), Δm = mass loss (%)].

Table 2. Experimental and calculated mass losses in % for compounds **1-Mn** and **2-Mn**.

— **1-Mn** —		— **2-Mn** —	
Δm_{exp} (1st step)	48.1	Δm_{exp} (1st step)	6.3
Δm_{calc} (−2 bpe)	50.7	Δm_{calc} (−2 H_2O)	6.3
Δm_{exp} (2nd step)	35.7	Δm_{exp} (2nd step)	31.9
Δm_{calc} (−1 bpe)	25.4	Δm_{calc} (−1 bpe)	31.8

the ligand-rich 1 : 2 hydrate $Mn(NCS)_2(bpe)_2(H_2O)_2$ (**2-Mn**) were investigated for their thermal properties using simultaneous differential thermoanalysis and thermogravimetry, elemental analysis and powder X-ray diffraction. On heating the 1 : 3 compound **1-Mn**, two distinct mass steps are observed in the TG curve, which are accompanied by endothermic events in the DTA curve (Fig. 4). The experimental mass losses of the first heating steps are in reasonable agreement with those calculated for the removal of two bpe molecules, whereas the mass loss in the second TG step does not agree well with that calculated for the removal of the remaining bpe ligand (Table 2). In contrast, if the hydrate 1 : 2 is heated, three mass steps are observed that are accompanied with three endothermic events in the DTA curve. The experimental mass loss in the first TG step is in perfect agreement with that calculated for the loss of two water molecules, and the mass loss in the second TG step is in accordance with that calculated for the removal of half of the bpe ligand (Fig. 4, Table 2). On further heating, the corresponding metal thiocyanate forms in a separate step, and decomposes at higher temperatures.

Based on these results it can be assumed that compound **1-Mn** is transformed in the first TG step into a ligand-deficient compound of composition $[Mn(NCS)_2(bpe)]_n$ (**4-Mn**), whereas **2-Mn** forms an anhydrate (**3-Mn**) in the first and the 1 : 1 compound **4-Mn** in the second TG step. To prove these assumptions, additional TG measurements were performed up to the first and second heating step, respectively. The residues obtained were investigated by elemental analysis (see Experimental Section). These investigations have clearly shown that in the first step a ligand-rich anhydrous 1 : 2 compound **3-Mn** was formed and that in the second step, and also in the first step of compound **1-Mn**, the ligand-deficient 1 : 1 compound **4-Mn** is obtained.

In order to determine the coordination mode of the thiocyanato anions in all compounds, the CN stretching vibrations of the anions were determined by IR spectroscopy (Table 3). From IR data it is obvious that in comparison to the ligand-rich 1 : 3 complex $[Mn(NCS)_2(bpe)_2{\cdot}(bpe)]$ (**1-Mn**) and the 1 : 2 complex $Mn(NCS)_2(bpe)_2(H_2O)_2$ (**2-Mn**) the CN bands in **4-Mn** are shifted to values above 2100 cm^{-1} which indicates the presence of μ-1,3-bridging thiocyanato anions (Table 3) [26, 27]. In the IR spectra of the anhydrate **3-Mn** two different bands at 2094 and 2054 cm^{-1} were observed and therefore, the coordination mode of the thiocyanato anions cannot unambiguously be determined.

Table 3. Values of the characteristic CN stretching vibrations of the thiocyanato anion for compounds **1-Mn** to **4-Mn**. For full IR data see Experimental Section.

Compound	Formula	ν_{max} (CN) (cm^{-1})
1-Mn	$[Mn(NCS)_2(bpe)_2{\cdot}(bpe)]$	2053
2-Mn	$[Mn(NCS)_2(bpe)_2(H_2O)_2]$	2058
3-Mn	$[Mn(NCS)_2(bpe)_2]$	2094 / 2054
4-Mn	$[Mn(NCS)_2(bpe)]_n$	2105

Based on the results mentioned above we tried to prepare the anhydrate **3-Mn** as well as the ligand-deficient 1 : 1 compound **4-Mn** in solution. However, independent of the reaction conditions the anhydrate could not be prepared, and only either the 1 : 3 compound **1-Mn** or the hydrate **2-Mn** was obtained. In contrast, if an excess of the metal salt is used, **4-Mn** can be obtained as crystals suitable for single-crystal structure determination using solvothermal conditions.

*Crystal structure of $[Mn(NCS)_2(bpe)]_n$ (**4-Mn**)*

Compound $[Mn(NCS)_2(bpe)]_n$ (**4-Mn**) crystallizes in the centrosymmetric triclinic space group $P\bar{1}$ with two formula in the unit cell [24]. The asymmetric unit consists of two manganese(II) cations located on centers of inversion and two thiocyanato anions in general positions as well as two bpe ligands which are located on a center of inversion. The manganese(II) cations are coordinated by two *N*- and two *S*-bonded thiocyanato anions as well as two *N*-bonded bpe ligands in an octahedral coordination mode (Fig. 5: top). The MnN_4S_2 octahedron is slightly distorted with bond lengths between 2.138(5) and 2.7081(15) Å. The angles around the manganese(II) cations are in the range from 85.00(12) to 180.0 ° (Table 4).

The manganese(II) cations are linked into chains by μ-1,3 bridging thiocyanato anions, which is in agreement with the IR data (see above). These Mn-$(NCS)_2$-Mn chains are connected by the bpe ligand into layers (Fig. 5: bottom). Within the chain the dihedral angle between the neighboring pyridine rings (N1–C5 and N11–C15) amounts to 111.4 °.

Table 4. Selected bond lengths (Å) and angles (deg) for compound **4-Mn**.

Mn1–N21	2.138(5)	Mn2–N31	2.154(4)
Mn1–N1	2.265(4)	Mn2–N11	2.272(4)
Mn1–S31B	2.705(1)	Mn2–S21	2.708(1)
N21A–Mn1–N21	180	N31–Mn2–N11B	90.37(17)
N21A–Mn1–N1	90.11(17)	N31–Mn2–N11	89.63(17)
N21–Mn1–N1	89.89(17)	N11B–Mn2–N11	180
N1A–Mn1–N1	180	N31–Mn2–S21	85.00(12)
N21A–Mn1–S31B	87.35(12)	N11B–Mn2–S21	90.36(13)
N21–Mn1–S31B	92.65(12)	N11–Mn2–S21	89.64(13)
N1–Mn1–S31B	90.17(12)	N31–Mn2–S21B	95.00(12)
N1–Mn1–S31C	89.83(12)	N31B–Mn2–N31	180
N2–Mn1–N61	91.76(12)	N11–Mn2–S21B	90.36(13)

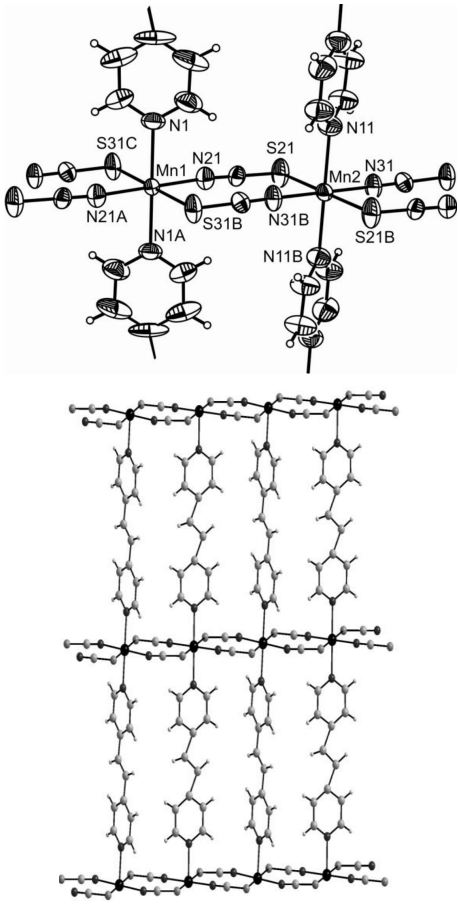

Fig. 5. Molecular structure of **4-Mn** with atom labeling adopted and displacemant ellipsoids drawn at 50 % probability level (top; ORTEP). View of the crystal structure of **4-Mn** onto the layers (bottom). Symmetry codes: A = $-x$, $-y+1$, $-z$; B = $-x+1$, $-y+2$, $-z+1$; C = $x-1$, $y-1$, $z-1$. For clarity only a part of the bpe ligands is shown.

Based on the structural data for **4-Mn**, a powder X-ray pattern was calculated and compared with those

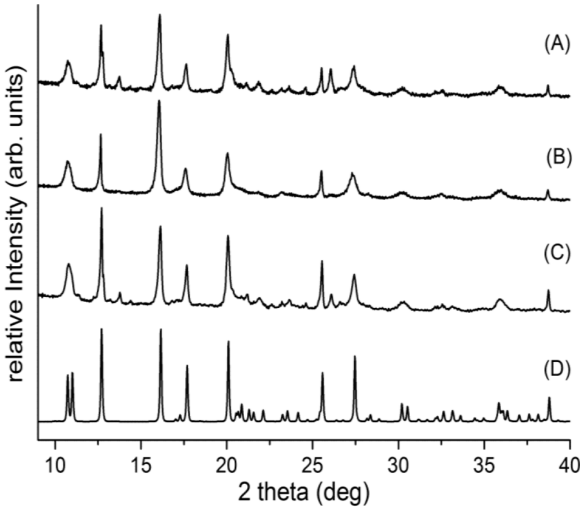

Fig. 6. Experimental powder X-ray diagrams of the residues isolated after the first (A) or second mass loss (B) in the TG measurements of **1-Mn** and **2-Mn** together with the experimental powder diagram of the sample obtained from solution (C), and the powder X-ray diagram for compound **4-Mn** as calculated from single-crystal data (D).

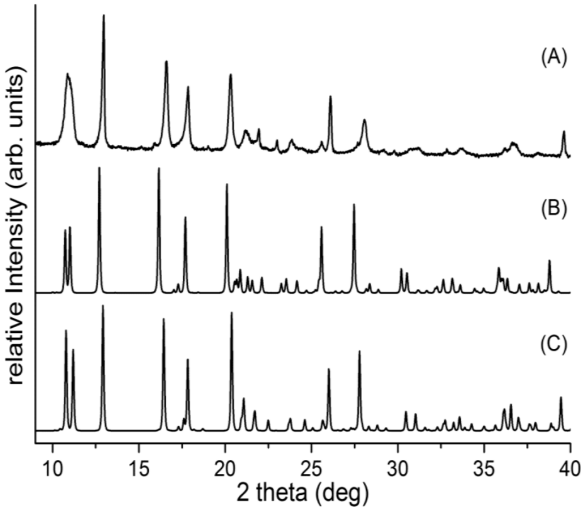

Fig. 7. Experimental powder X-ray diagram of the ligand-deficient 1 : 1 compound **1-Ni** (A), powder diagram as calculated from single-crystal data for **4-Mn** (B), and a diagram based on the results of a Rietveld refinement for **1-Ni** (C).

measured for the residues obtained in the thermal decomposition reactions of **1-Mn** and **2-Mn** as well as for the sample obtained from solution. The results prove that always the same compound is obtained phase-pure that corresponds to the 1 : 1 compound **4-Mn** (Fig. 6).

In further experiments we tried to prepare similar compounds based on nickel(II) thiocyanate and

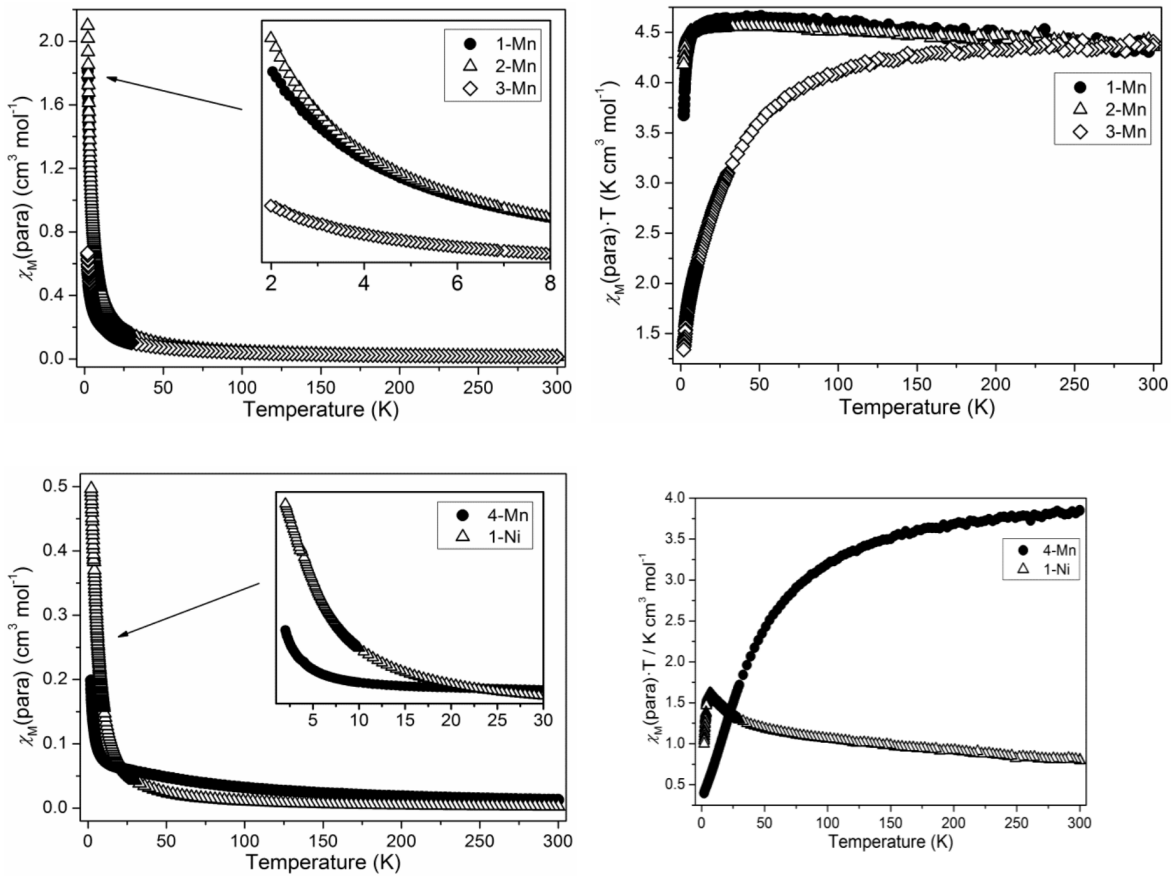

Fig. 8. Paramagnetic susceptibility (left) and $\chi_M T$ (right) as a function of temperature for the ligand-rich compounds $[Mn(NCS)_2(bpe)_2 \cdot (bpe)]$ (**1-Mn**), $Mn(NCS)_2(bpe)_2(H_2O)_2$ (**2-Mn**), and $[Mn(NCS)_2(bpe)_2]$ (**3-Mn**), as well as for the ligand-deficient compounds $[Mn(NCS)_2(bpe)]_n$ (**4-Mn**) and $[Ni(NCS)_2(bpe)]_n$ (**1-Ni**). The insets show measurements in the low-temperature range.

bpe. Surprisingly, independently of the reaction conditions always only one crystalline phase of composition $[Ni(NCS)_2(bpe)]_n$ (**1-Ni**) was obtained, which is isotypic to **4-Mn** (Fig. 7). Therefore, based on the crystallographic data of **4-Mn** the lattice parameters were refined for **1-Ni** using a Rietveld refinement. The resulting unit cell parameters are: a = 9.3108(10), b = 9.4980(10), c = 10.4218(10) Å, α = 113.71(5), β = 110.37(6), γ = 93.55(20)°, V = 768.89(14) Å^3. When the experimental pattern of **1-Ni** is compared with that calculated from the Rietveld refinement, it becomes obvious that **1-Ni** was obtained as a phase-pure material (Fig. 7).

Magnetic properties

All compounds were investigated for their magnetic properties, and the temperature dependence of their susceptibility was investigated applying a magnetic field of H_{DC} = 1 kOe (1 kOe = 7.96×10^4 A m^{-1}) in the temperature range of 300 – 2 K (Fig. 8). In compounds **1-Mn** and **2-Mn** the thiocyanato anions are only terminally bonded, and the paramagnetic manganese(II) cations are only connected by the organic ligand *trans*-1,2-bis(4-pyridyl)ethylene (bpe). Therefore, only Curie- or Curie-Weiss paramagnetism are expected. For the anhydrate **3-Mn** the situation is more

Table 5. Results of the magnetic measurements for all compounds.

Compound	**1-Mn**	**2-Mn**	**3-Mn**	**4-Mn**	**1-Ni**
C, cm^3 K mol^{-1}	4.41	4.41	4.56	4.29	0.94
θ, K	0.98	0.69	−11.44	−34.71	4.61
μ_{eff}(exp), μ_B	5.93	5.94	6.03	5.86	2.74
μ_{eff}(calcd), μ_B	5.92	5.92	5.92	5.92	2.82
Fit range, K	2 – 300	2 – 300	40 – 300	50 – 300	2 – 200

complex because the coordination mode of the anions cannot unambiguously be determined, but from simple coordination chemical considerations it can be assumed that terminal anions are present. In contrast, in compounds **4-Mn** and **1-Ni** the metal centers are connected by μ-1,3 bridging ligands which could enable cooperative magnetic phenomena. However, for all compounds only Curie-Weiss paramagnetism is found (Fig. 8, Table 5). Fitting the magnetic data according to the Curie-Weiss law $\chi_M = C/(T-\theta)$ gives no evidence of significant interactions in **1-Mn**, **2-Mn** and **1-Ni**, but indicates stronger antiferromagnetic exchange interactions for **3-Mn** and **4-Mn** (Table 5). In agreement with these findings the $\chi_M T$ values for **4-Mn** decrease continuously. For **1-Ni** ferromagnetic exchange interactions are found, and on cooling the $\chi_M T$ values increase reaching a maximum at about 6.9 K (Fig. 8). The effective magnetic moments μ_{eff} are in good agreement with the spin-only value for a high-spin Mn(II) cation (S = 5/2, g = 2) and for a high-spin Ni(II) cation (S = 1, g = 2), respectively.

The fact that no cooperative magnetic phenomena are observed for the μ-1,3-bridged compounds is somehow surprising because we reported recently on the structure and magnetic properties of $[Mn(NCS)_2(pyridine)_2]_n$ in which the manganese cations are also connected by μ-1,3-bridging thiocyanato anions. For this compound a similar value for the Weiss constant is found as for **4-Mn** (θ = −37.4 K) but this compound shows antiferromagnetic ordering at T_N = 23.5 K [28]. Moreover, the corresponding Ni compound shows metamagnetic behavior with an antiferromagnetic ordering at T_N = 3.9 K below and ferromagnetic ordering (T_C = 4.2 K) above the critical field of 0.6 T [28]. These differences are difficult to explain but indicate that the bpe ligand may participate in the magnetic exchange interactions in **4-Mn** and **1-Ni**.

Conclusion

To summarize, in this contribution we have presented several new coordination polymers on the basis of Mn and Ni thiocyanate and bpe as a neutral ligand. On heating, compounds **1-Mn** and **2-Mn** lose some of the neutral ligands and are transformed into the ligand-deficient 1 : 1 coordination polymer $[Mn(NCS)_2(bpe)]_n$ (**4-Mn**), which can also be obtained in solution. Therefore, these results are similar to those obtained for the corresponding compounds with Co(II) reported recently [24]. In contrast, with Ni(II) only one compound of composition $[Ni(NCS)_2(bpe)]_n$ (**1-Ni**) was obtained which is isotypic to **4-Mn**, and there are no hints for the formation of more bpe-rich compounds or hydrates. Magnetic investigations have revealed that for all compounds Curie- or Curie-Weiss paramagnetism is observed independent if the metal cations are coordinated only by *N*-terminal thiocyanato anions or if they are μ-1,3 bridged by the anionic ligands.

Experimental Section

$MnCl_2 \cdot 2H_2O$, $Ni(NCS)_2$ and KNCS as well as $MnSO_4 \cdot H_2O$ and $Ba(NCS)_2 \cdot 3H_2O$ were obtained from Alfa Aesar, *trans*-1,2-bis(4-pyridyl)ethylene was obtained from Sigma Aldrich. All chemicals were used without further purification. $Mn(NCS)_2 \cdot H_2O$ was prepared by a reaction of equimolar amounts of $MnSO_4 \cdot H_2O$ and $Ba(NCS)_2 \cdot 3H_2O$ in water. The resulting precipitate of $BaSO_4$ was filtered off, and the filtrate was concentrated to complete dryness resulting in a beige residue of $Mn(NCS)_2 \cdot H_2O$. The purity was checked by XRPD and elemental analysis. All crystalline powders were prepared by stirring the reactants in solution for 3 d at r. t. The residues were filtered off and washed with water and diethyl ether and dried in air.

*Preparation of $[Mn(NCS)_2(bpe)_2 \cdot (bpe)]$ (**1-Mn**)*

Single crystals suitable for X-ray structure determination were obtained by a reaction of $Mn(NCS)_2 \cdot H_2O$ (27.8 mg, 0.15 mmol), *trans*-1,2-bis(4-pyridyl)ethylene (160.7 mg, 0.9 mmol) and 1 mL water in a closed test tube at 120 °C. Yellow block-shaped single crystals grew on cooling after 3 d.

A yellow crystalline powder was obtained by the reaction of $MnCl_2 \cdot 2\ H_2O$ (27.1 mg, 0.15 mmol) and KNCS (31.2 mg, 0.3 mmol) mixed with *trans*-1,2-bis(4-pyridyl)-ethylene (113.2 mg, 0.6 mmol) in 1 mL acetonitrile. Yield based on $MnCl_2 \cdot 2\ H_2O$: 98.7 mg (91.7 %). – Elemental analysis for $C_{38}H_{30}MnN_8S_2$ (717.77): calcd. C 63.59, H 4.21, N 15.61, S 8.93; found C 63.18, H 4.18, N 15.79, S 8.89. – IR (KBr): ν = 3423 (br), 3029 (w), 2053 (s), 1604 (s), 1414 (w), 1211 (w), 1010 (w), 964 (m), 832 (w), 551 (m) cm^{-1}.

*Preparation of $Mn(NCS)_2(bpe)_2(H_2O)_2$ (**2-Mn**)*

A yellow crystalline powder was prepared by the reaction of $MnCl_2 \cdot 2\ H_2O$ (41.5 mg, 0.25 mmol), KNCS (51.1 mg, 0.5 mmol) and *trans*-1,2-bis(4-pyridyl)ethylene (91.0 mg, 0.5 mmol) in a mixture of 1.5 mL water and 1.5 mL ethanol. Yield based on bpe: 130.2 mg (91.1 %). – Elemental analysis for $C_{26}H_{24}MnN_6S_2O_2$ (571.58): calcd. C 54.64, H 4.23, N 14.70, S 11.22; found C 54.32, H 4.09, N 14.52, S 11.35. – IR (KBr): ν = 3420 (br), 2858 (w), 2058 (s), 1647 (w), 1607 (s), 1600 (s), 1558 (w), 1502 (w), 1425 (m), 1220 (w),

1012 (m), 971 (m), 839 (w), 825 (m), 647 (w), 549 (m), 479 (w) cm^{-1}.

*Preparation of $[Mn(NCS)_2(bpe)_2]_n$ (**3-Mn**)*

This compound cannot be prepared in solution. However, a light-yellow crystalline powder of **3-Mn** was obtained as a residue in the first TG step of the thermal decomposition reaction of compound **2-Mn** (see Thermal Reactivity). – Elemental analysis for $C_{26}H_{20}MnN_6S_2$ (535.56): calcd. C 58.31, H 3.76, N 15.69, S 11.97; found C 58.36, H 3.66, N 15.83, S 11.74. – IR (KBr): ν = 3410 (br), 3027 (w), 2094 (s), 2054 (s), 1604 (s), 1555 (w), 1502 (w), 1424 (m), 1218 (w), 1213 (w), 1067 (w), 1011 (m), 971 (m), 826 (m), 561 (m), 469 (w) cm^{-1}.

*Preparation of $[Mn(NCS)_2(bpe)]_n$ (**4-Mn**)*

Single crystals suitable for X-ray structure determination were obtained by the reaction of $MnCl_2{\cdot}2\ H_2O$ (52.8 mg, 0.3 mmol), KNCS (61.9 mg, 0.6 mmol) and *trans*-1,2-bis(4-pyridyl)ethylene (28.9 mg, 0.15 mmol) as well as 1 mL ethanol in a closed test tube at 120 °C. Yellow block-shaped single crystals grew on cooling after 3 d.

A yellow crystalline powder was prepared by the reaction of $Mn(NCS)_2{\cdot}H_2O$ (38.0 mg, 0.2 mmol) and *trans*-1,2-bis-(4-pyridyl)ethylene (40.4 mg, 0.2 mmol) in 1 mL methanol. Yield based on bpe: 62.4 mg (88.3 %). – Elemental analysis for $C_{14}H_{10}MnN_4S_2$ (353.33): calcd. C 47.59, H 2.85, N 15.86, S 18.15; found C 47.99, H 3.00, N 16.03, S 18.39. – IR (KBr): ν = 2105 (s), 2093 (s), 1605 (s), 1425 (m), 1219 (w), 1012 (m), 827 (m), 553 (m) cm^{-1}.

*Preparation of $[Ni(NCS)_2(bpe)]_n$ (**1-Ni**)*

A light-green crystalline powder was prepared by the reaction of $Ni(NCS)_2$ (25.8 mg, 0.15 mmol) and *trans*-1,2-bis-(4-pyridyl)ethylene (28.7 mg, 0.15 mmol) in 1 mL water. Yield based on bpe: 50.72 mg (94.7 %). – Elemental analysis for $C_{14}H_{10}NiN_4S_2$ (357.08): calcd. C 47.09, H 2.89, N 15.69, S 17.96; found C 48.28, H 2.95, N 15.97, S 17.82. – IR (KBr): ν = 3436 (br), 3062 (w), 2909 (w), 2126 (s), 2120 (s), 1607 (s), 1503 (m), 1425 (m), 1217 (m), 1066 (m), 1017 (m), 970 (m), 828 (m), 556 (s), 470 (w) cm^{-1}.

*Results of the elemental analysis and IR spectroscopy of the residues obtained on thermal decomposition of compounds **1-Mn** and **2-Mn***

Material isolated after the first TG step of **1-Mn**: Elemental analysis for $C_{14}H_{10}MnN_4S_2$ (353.33): calcd. C 47.59, H 2.85, N 15.86, S 18.15; found C 47.57, H 2.87, N 15.77, S 17.97. – IR (KBr): ν = 2098 (s), 1607 (s), 1503 (w), 1426 (m), 1204 (w), 1066 (w), 1016 (m), 970 (m), 829 (m), 553 (m) cm^{-1}.

Table 6. Selected crystal data and results of the structure refinement for **1-Mn** and **4-Mn**.

Compound	**1-Mn**	**4-Mn**
Formula	$C_{38}H_{30}MnN_8S_2$	$C_{14}H_{10}MnN_4S_2$
Crystal system	triclinic	triclinic
M_r	717.76	353.32
Crystal size, mm^3	0.15×0.21×0.26	0.06×0.09×0.13
Space group	$P\bar{1}$	$P\bar{1}$
a, Å	14.0199(6)	9.4867(9)
b, Å	14.0431(6)	9.5901(8)
c, Å	19.3706(9)	10.5049(9)
α, deg	71.245(3)	112.929(6)
β, deg	82.224(4)	110.488(7)
γ, deg	86.512(4)	93.762(7)
V, $Å^3$	3577.4(3)	801.61(12)
T, K	293(2)	293(2)
Z	4	2
D(calcd), g cm^{-3}	1.33	1.46
F(000), e	1484	358
μ, mm^{-1}	0.5	1.1
Transmission (min / max)	0.804 / 0.874	0.828 / 0.902
θ_{max}, deg	25.74	26.00
Reflections collected	44298	7508
Independent reflections / R_{int}	13487 / 0.0679	3125 / 0.0420
Reflections with $I \geq 2\sigma(I)$	9155	2007
Restraints / ref. parameters	0 / 883	0 / 198
Final $R1$ [$I \geq 2\sigma(I)$] / $wR2$ (all data)	0.0729 / 0.1350	0.0587 / 0.1389
Goodness-of-fit on F^2	1.154	1.066
$\Delta\rho_{fin}$ (max / min), e $Å^{-3}$	0.29 / −0.33	0.59 / −0.28

Material isolated after the first TG step of **2-Mn**: Elemental analysis for $C_{26}H_{20}MnN_6S_2$ (535.56): calcd. C 58.31, H 3.76, N 15.69, S 11.97; found C 58.36, H 3.66, N 15.83, S 11.74. – IR (KBr): ν = 3410 (br), 3027 (w), 2094 (s), 2054 (s), 1604 (s), 1555 (w), 1502 (w), 1424 (m), 1218 (w), 1213 (w), 1067 (w), 1011 (m), 971 (m), 826 (m), 561 (m), 469 (w) cm^{-1}.

Material isolated after the second TG step of **2-Mn**: Elemental analysis for $C_{14}H_{10}MnN_4S_2$ (353.33): calcd. C 47.59, H 2.85, N 15.86, S 18.15; found C 47.40, H 2.69, N 15.48, S 17.85. – IR (KBr): ν = 3428 (br), 2092 (s), 1606 (s), 1504 (m), 1426 (m), 1218 (w), 1066 (w), 1012 (m), 971 (m), 828 (m), 553 (m) cm^{-1}.

Powder X-ray diffraction

The experiments were performed using a PANalytical X'Pert Pro MPD Reflection Powder Diffraction System with Cu$K_{\alpha 1}$ radiation (λ = 154.0598 pm) equipped with a PIXcel semiconductor detector from PANalytical.

Simultaneous differential thermoanalysis and thermogravimetry (DTA-TG)

The thermal decomposition reactions were performed in an atmosphere of nitrogen (purity: 5.0) in Al_2O_3 crucibles

using a STA-409CD thermobalance from Netzsch. All measurements were performed with a flow rate of 75 mL min^{-1} and a heating rate of 4 K min^{-1}. The instrument was calibrated using standard reference materials.

IR spectroscopy

All IR data were obtained using an ATI Mattson Genesis Series FTIR Spectrometer, control software: WINFIRST, from ATI Mattson.

Magnetic measurement

Magnetic measurements were performed using a Physical Property Measurement System (PPMS) from Quantum Design, which is equipped with a 9 T magnet. The data were corrected for core diamagnetism.

Elemental analysis

CHNS analyses were performed in a Euro EA Elemental Analyzer from Eurovector.

Single-crystal structure analyses

Single-crystal data collections were carried out on an imaging plate diffraction system (Stoe IPDS-1) with MoK_α radiation. The structures were solved with Direct Methods using SHELXS-97, and structure refinements were performed against F^2 using SHELXL-97 [29]. Numerical absorption correction was applied using the programs X-RED and X-SHAPE of the program package X-AREA [30]. All non-hydrogen atoms were refined with anisotropic displacement parameters. All hydrogen atoms were positioned with idealized geometry and were refined with isotropic displacement parameters [U_{eq}(H) = $-1.2U_{eq}$(C)] by using a riding model with $d_{C\text{-}H}$ = 0.93 Å for **1-Mn** and **4-Mn**. In **1-Mn** one C atom of the bpe ligand is disordered and was refined using a split model. Details of the structure determinations are given in Table 6. The crystal of **4-Mn** was non-merohedrally twinned and therefore, a twin refinement was performed [matrix: 0 1 0 1 0 0 0 0 1; BASF parameter: 0.106(6)]. Further details of the structure determinations are summarized in Table 6.

CCDC 859190 (**1-Mn**) and CCDC 859191 (**4-Mn**) contain the supplementary crystallographic data for this paper. These data can be obtained free of charge from The Cambridge Crystallographic Data Centre *via* http://www.ccdc.cam.ac.uk/data_request/cif.

Acknowledgements

We thank Professor Dr. W. Bensch for access to his experimental facilities. This project was supported by the Deutsche Forschungsgemeinschaft (Project No. Na 720/3-1) and the State of Schleswig Holstein.

[1] G. Férey, *Dalton Trans.* **2009**, 4400.
[2] G. Férey, C. Serre, *Chem. Soc. Rev.* **2009**, *38*, 1380.
[3] S. Kitagawa, R. Matsuda, *Coord. Chem. Rev.* **2007**, *251*, 2490.
[4] C. Janiak, *Dalton Trans.* **2003**, 2781.
[5] D. Maspoch, D. Ruiz-Molina, J. Veciana, *J. Mater. Chem.* **2004**, *14*, 2713.
[6] J. S. Miller, *Dalton Trans.* **2006**, 2742.
[7] E. Pardo, R. Ruiz-Garcia, J. Cano, X. Ottenwaelder, R. Lescouezec, Y. Journaux, F. Lloret, M. Julve, *Dalton Trans.* **2008**, 2780.
[8] A. Prescimone, J. Wolowska, G. Rajaraman, S. Parsons, W. Wernsdorfer, M. Murugesu, G. Christou, S. Piligkos, E. J. L. McInnes, E. K. Brechin, *Dalton Trans.* **2007**, 5282.
[9] H. N. Bordallo, L. Chapon, J. L. Manson, C. D. Ling, J. S. Qualls, D. Hall, D. N. Argyriou, *Polyhedron* **2003**, *22*, 2045.
[10] M. Julve, M. Verdaguer, G. Demunno, J. A. Real, G. Bruno, *Inorg. Chem.* **1993**, *32*, 795.
[11] T. Rojo, R. Cortes, L. Lezama, M. I. Arriortua, K. Urtiaga, G. Villeneuve, *J. Chem. Soc., Dalton Trans.* **1991**, 1779.
[12] R. Vicente, A. Escuer, E. Penalba, X. Solans, M. Font-Bardia, *Inorg. Chim. Acta* **1997**, *255*, 7.
[13] R. Vicente, A. Escuer, J. Ribas, X. Solans, *J. Chem. Soc., Dalton Trans.* **1994**, 259.
[14] M. Wriedt, C. Näther, *Z. Anorg. Allg. Chem.* **2009**, *635*, 2459.
[15] M. Wriedt, C. Näther, *Dalton Trans.* **2010**, *40*, 886.
[16] M. Wriedt, C. Näther, *Chem. Commun.* **2010**, *46*, 4707.
[17] J. Boeckmann, M. Wriedt, C. Näther, *Eur. J. Inorg. Chem.* **2010**, 1820.
[18] J. Boeckmann, C. Näther, *Dalton Trans.* **2010**, *39*, 11019.
[19] J. Boeckmann, C. Näther, *Chem. Commun.* **2011**, *47*, 7104.
[20] M. Wriedt, C. Näther, *Z. Anorg. Allg. Chem.* **2009**, *635*, 1115.
[21] M. Wriedt, C. Näther, *Eur. J. Inorg. Chem.* **2011**, *2011*, 228.
[22] M. Wriedt, S. Sellmer, C. Näther, *Inorg. Chem.* **2009**, *48*, 6896.
[23] M. Wriedt, S. Sellmer, C. Näther, *Dalton Trans.* **2009**, 7975.
[24] S. Wöhlert, J. Boeckmann, M. Wriedt, C. Näther, *Angew. Chem.* **2011**, *123*, 7053; *Angew. Chem. Int. Ed.* **2011**, *50*, 6920.
[25] A. Briceno, Y. Hill, T. Gonzalez, G. D. d. Delgado, *Dalton Trans.* **2009**, 1602.

[26] L. Shen, Y.-Z. Xu, *J. Chem. Soc., Dalton Trans.* **2001**, 3414.
[27] G. A. Van Albada, R. A. G. De Graaff, J. G. Haasnoot, J. Reedijk, *Inorg. Chem.* **1984**, *23*, 1404.
[28] J. Boeckmann, C. Näther, *Polyhedron* **2011**; 10.1016/j.poly.2011.10.013.
[29] G. M. Sheldrick, *Acta Crystallogr.* **2008**, *A64*, 112.
[30] X-RED (version 1.11), X-SHAPE (version 1.03), Crystal Optimization for Numerical Absorption Correction, Stoe & Cie GmbH, Darmstadt (Germany) **1998**.